Experimental and numerical study on a gasoline surrogate mixture

Outmane Mghanen[1,2], Michael Matrat[3], Roland Dauphin[1], Anthony Robert[3], Stephane Chevillard[3], Nicolas Obrecht[1], Nabiha Chaumeix[2]
[1]Centre de Recherches de Solaize TotalEnergies, chemin du canal, Solaize, France
[2] Institut de Combustion, Aérothermique, Réactivité et Environnement, CNRS, Orleans, France
[3] IFP Energies nouvelles, 1 et 4 avenue de Bois-Préau, Rueil-Malmaison, France

1 Introduction

Nowadays, the energy sector is in a state of transition and governments are more concerned about global greenhouse emissions and their environmental impact with regard to climate change. In 2016, the average concentration of CO2 equivalent was about 40% higher than 1990 levels [1]. This. study is directly related to the transport sector, it represents 15.9% of the global greenhouse gas emissions in 2016 [2]. In order to reach the net zero by 2050 (European union objective) all innovation and development efforts are mandatory and internal combustion engines still make sense for decades to come [3]. In Spark ignition engines, many developments are focused on downsizing or rightsizing methods in order to reduce fuel consumption and to increase engine efficiency. However, this technology promotes knock occurrence. As knock is related to fuel physical and chemical characteristics, developing knock resistant fuels helps take full advantage of the before mentioned technique. In this context, the objective of this work is to generate reliable laminar flame speed measurements for correlation development. Detailed mechanisms are often too large to perform laminar flame simulations for which convergence is rarely achieved. The alternative proposed in this work is to generate an experimental/numerical based flame speed correlation. The validated mechanism for ignition delay time and the correlation will help generate look up tables [4] to use for 3D CFD Simulations. The latter will be used to perform mono-parametric variations of fuel characteristics, impossible to achieve in real engine tests, using an advanced RANS methodology [5] in order to determine key-parameters regarding knock phenomena.

2 Materials and methods

The main fuel used in this study is composed of 79.57% mole fraction of Toluene and 20.43% mole fraction of 1-hexene. This composition has been specifically chosen because of its RON, MON properties and, more importantly, fuel octane sensitivity. Another reason behind the choice of these specific compounds is that their chemical kinetics models are widely developed in literature. This fuel of reference will be used to validate a global CFD methodology consisting of evaluating fuel physical and chemical properties regarding knock occurrence. The spherical bomb used in the current study for laminar flame speed measurements was described in previous studies [6, 7, 8]. The current experimental study was conducted at two initial temperatures, 375 and 475 K ($\Delta T_u = \pm 1\ K$). Equivalence ratios are ranging from 0.7 to 1.2 ($\Delta\varphi =$

Correspondence to: outmane.mghanen@cnrs-orleans.fr

$\pm 0.07\%$), at a pressure of 1 bar ($\Delta P = \pm 0.14\ mbar$). Figure 1 exemplifies the flames recorded are spherical smooth and only very minor cracks can be observed on the surface of the flame due to the presence of the electrodes.

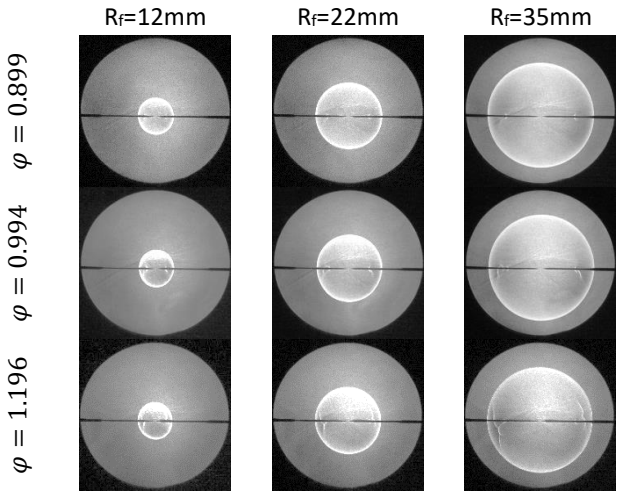

Figure 1: A series of flame snapshots for different flame radii and at different equivalence ratios. The mixture is constituted of {20.43% 1-Hexene + 79.57% Toluene}/air at 1 bar and 375K.

Eschenbach and Agnew [9] have given the expression of laminar flame velocity at zero stretch: $S_L^0 = \frac{V_s^0}{\sigma}\ with\ \sigma = \frac{\rho_u}{\rho_b}$ where ρu and ρb are respectively the density of fresh and burned gases at equilibrium. Once Vs0 is determined the previous equation is used to calculate the laminar flame speed. The spatial velocity is then calculated with the following equation Vs = (dRf)/dt. Nevertheless, the spherical shape of the flame must be considered because the curvature of the latter induces a stretch. The stretch is defined by the equation1: $\kappa = 2 * (V_s/R_f)$ Where κ is the stretch, Rf the radius of the spherical flame and Vs the spatial velocity. Subsequently, Ronney and Sivashinsky [10] have shown that for a weak stretch, a non-linear relationship exists between laminar flame velocity and stretching: $\left(\frac{V_s}{V_s^0}\right)^2 Ln\left(\frac{V_s}{V_s^0}\right)^2 = -2.(L_b.\frac{\kappa}{V_s^0})$ In fact, a linear relation leads to an overestimation of $Vs0$. The points extracted from image processing can be used to calculate the spatial velocity at zero stretch and consequently the laminar flame speed. However, the stretch induced by flame propagation affects the laminar flame speed calculated value. [11] presented non-linear formulations relating spatial velocity to the stretch. The curve of the spatial velocity is plotted as a function of the stretch Figure 2(a)

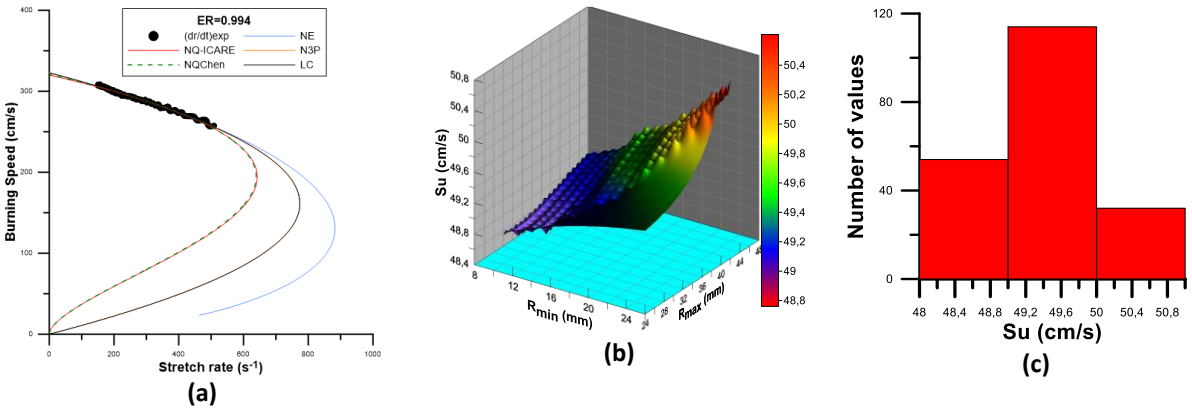

Figure 2: (a) Flame speed as a function of stretch of {20.43% 1-Hexene + 79.57% Toluene}/air at 1 bar, 375K and an equivalence ratio of 0.994; (b) Su values 3D mapping, (c): distribution of Su values.

Where LS [12] is a linear model based on stretch, LC [13] is a linear model based on curvature, NE [14] is a non-linear model on expansion form, N3P [11] is a non-linear model with 3 fitting parameters, NQ [15]

is a quasi-steady non-linear model and finally, NQ-ICARE and NQchen are NQ solutions using respectively ICARE ODE [16] and linear regression. The filled points represent smooth data considered in building up the different models and only points acquired at a constant pressure were considered. The data fits well with the different linear and non-linear approaches. However, the V0 values are different at zero stretch. ICARE and Chen ODE have nearly similar V0 values, ICARE ODE was chosen to calculate flame speed at zero stretch. For each extrapolation, a specified minimum and maximum flame radius were defined for illustration purpose. A mis-choice of the radii range for flame speed extraction can lead to additional error. In order to avoid this, the extrapolation method is performed for various minimum radii ranging from 10 to 25 mm, and maximum radii ranging from 25 to 45mm with a 1mm step for both radii and a constraint of 15mm between the two values. For each maximum and minimum, radii flame speed at zero stretch is determined. Figure 2(b) represents a 2D mapping of flame speed values as function of minimum and maximum radii. 200 values were considered, as a result the mean laminar flame speed value for this specific example is 49,4 cm/s with a standard deviation of 0.5cm/s as a result the error is about two times the standard deviation which is less than 2%.

3 Experimental results

3.1 Laminar flame speed and Markenstein length

Wu et al. [17] showed that in order to minimize extrapolation errors, experiments should be conducted in the range of $-0.05 < Ma_{linear}.Ka_{middle} < 0.15$ as it is shown in Figure 3(c) results are within these limits. The Markstein length was determined using the same methodology for laminar flame speed using the linear model, whilst Karlovitz number was determined at the middle of the domain considered for flame speed extrapolation. Furthermore, Radiative heat losses lead to a decrease of the fame speed value. The equation proposed in [18] was used to calculate the radiation-corrected fame speed. Figure 3(a) illustrates the laminar flame speed mean values and the difference between the latter and the corrected values considering radiative effects. In this case study, two experimental conditions of 375K and 475K at 1atm have been chosen. The difference between the corrected value and the mean experimental one has a minimum near stochiometric conditions and a maximum in the rich and lean conditions. For 375K, the mean value is about 0.6 cm/s while for 475K the mean value is about 0.73 cm/s. these corrections are considered while comparing to mechanisms.

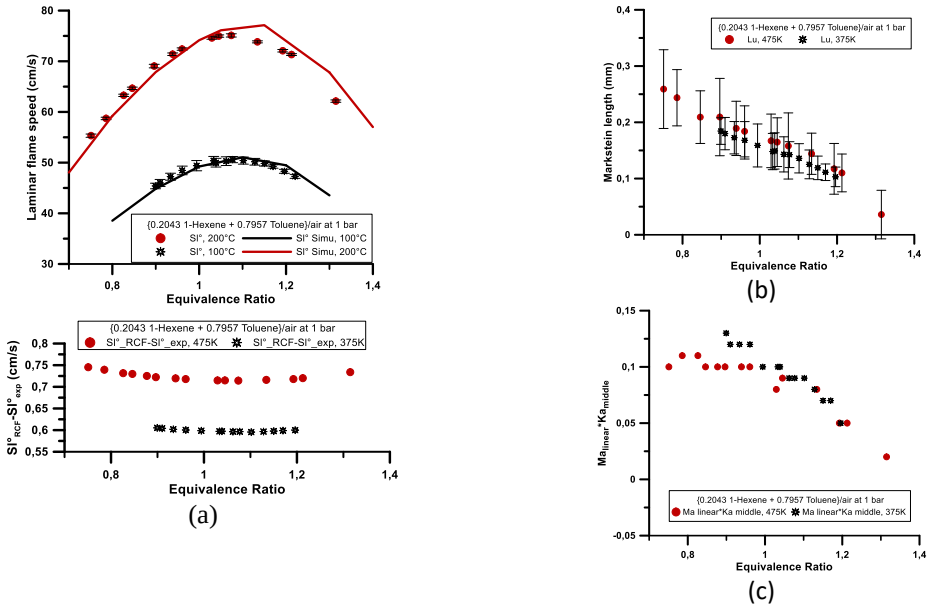

Figure 3: (a) Laminar flame speed measurements versus simulation; (b) Markenstein length; (c) $Ma_{linear}.Ka_{middle}$ parameter; all of {20.43% 1-Hexene + 79.57% Toluene}/air at 1 bar, 375K and 475K

The observations show that the laminar flame speed increases with higher temperatures. The resulting curve is parabolic, with an equivalence ratio range from 0.7 to 1.3 with a maximum value around the value of 1.07. The results obtained will be used to validate the mechanism used in building-up a numerical correlation for CFD usage. Using the Equation 3 the burned gases Markstein length Lb is calculated then the un- burned gases Markstein length L ' is determined using the following expression Lu = Lb/ σ. L' values are reported in Figure 3(b), one can see that for each initial condition on the entire range of equivalence ratio studied flames are stable (L' > 0). Lu values are nearly identical at iso-equivalence ratio which means that the initial temperature does not affect the response of the flame to the stretch.

3.2 Numerical simulation

The comparison between simulated Sl°obtained using the Polimi mechanism [19] and experimental data obtained is illustrated in Figure 3(a). The numerical solution is in good agreement with the experimental results in lean and stoichiometric conditions. While it overestimates the Sl0 value in rich conditions. The simulation work was performed using the premixed laminar flame speed calculation module in the Chemkin PRO software. A large computational domain of 10 cm was selected to avoid boundary effects. Very constrained grid parameters were used to ensure that the results obtained are grid-independent. Thus, the grid parameters used in this work are: GRAD: 0.05, CURV: 0.05 and a maximum grid point of 1800. The Soret diffusion effect and mixture averaged transport properties hypothesis was considered.

3.3 Correlation development

Numerical modeling of combustion plays a crucial role in optimizing processes and predicting physical and chemical behaviors. Although encouraging progress has been made in developing detailed chemical kinetic mechanisms, they are still extremely complex and require significant computational resources. Analytical correlations are more practical for industrial numerical usage. Various forms of empirical and semi-empirical functional relationships have been proposed for the laminar burning velocity [20] [21] [22]. The simplest and the most widely used form of the empirical correlation is the power law formula: $S_L^0(\varphi,T,P) = S_L^0(\varphi)\left(\frac{T}{T_0}\right)^{\alpha}\left(\frac{P}{P_0}\right)^{\beta}$ where $S_L^0(\varphi)$ is the laminar flame speed measured at $T = T_0$ and $P = P_0$. Gülder [21] proposed the following expression for $S_L^0(\varphi)$: $S_L^0(\varphi) = ZW\varphi^{\eta}e^{-\xi(\varphi-\sigma)^2}$ where Z = 1 for single constituent fuels. W, η, ξ and σ are constant for a given fuel. In the current study, the binary mixture is considered as a single component for correlation development. Liao et al. [23] have investigated the dependence of alpha and beta constant to the equivalence ratio. They proposed the following second-order polynomial form: $\alpha(\varphi) = a_2\varphi^2 - a_1\varphi + a_0$ and $\beta(\varphi) = -b_2\varphi^2 + b_1\varphi - b_0$. A new approach is used in order to build up a numerical correlation. It consists in combining experimental and numerical results obtained by computation using detailed mechanisms. The objective is to use a large sample of laminar flame speed values as an objective function to optimize the different correlation coefficients. First, W, η, ξ and σ are optimized to capture the equivalence ratio effect, thirteen experimental points at P0=1bar and T0=375K were fed to optimize the four coefficients. Figure 4(a) represent a comparison between correlation and experimental data. Coefficients values are reported in supplementary materials.

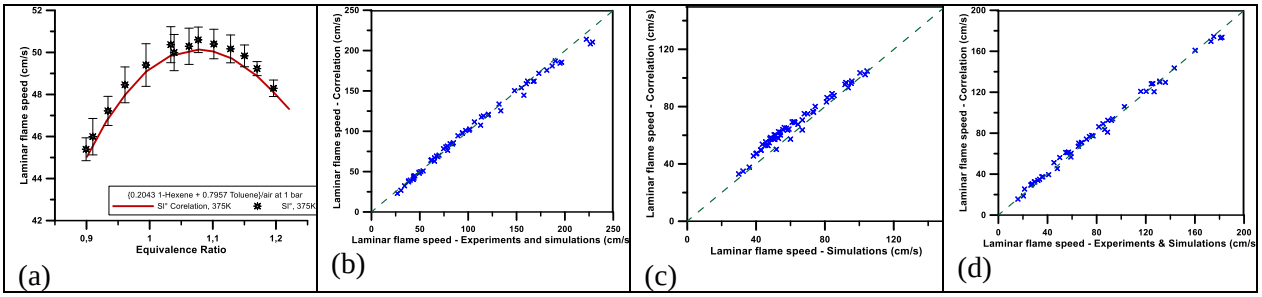

Figure 4: (a) Laminar flame speed correlation versus experimental data (b) Correlation results versus Experimental and simulation results, (c) Correlation results versus simulation using ChemkinPro (d) Correlation versus simulation and experimental data not used as an objective function.

The second step consists in fitting the temperature dependence coefficients. In order to do so, fifty-nine combined experimental and numerical SL values were chosen at 1bar, with temperature ranging from 350 to 800K and equivalence ration ranging from 0.7 to 1.3. The form of Liao et al. [23] of the coefficient alpha which represents the temperature dependence is considered. Figure 4(b) represents the correlation results versus the objective values. A correlation coefficient of 0.928 is obtained. The third and final step of the optimization is to capture the pressure dependence. The form of coefficient beta is also used from [23]. The database used contains fifty-six numerical SL values at 600K, ranging from 1 to 35 bar in terms of pressure. The optimization results are presented in Figure 4(c). A correlation coefficient of 0.907 is obtained. Finally, another database is used to validate the correlation results. It is composed of mixed experimental measurements and numerical calculations that were not used as an objective function, corresponding to conditions that were not covered by the optimization study. Fifty-one SL values are used and a correlation coefficient of 0.989 is obtained presented in Figure 4(d).

4 Conclusion

The aim of this study is to prepare the 3D CFD inputs in the most accurate way in terms of ignition delay time and laminar flame speed. New Laminar flame speed measurements were presented while highlighting the importance of well choosing an accurate minimum and maximum flame radius. A new 2D statistical approach is proposed for minimum and maximum radius selection. Furthermore, several mechanisms were analyzed for this specific fuel mixture. Polimi mechanism was chosen for laminar flame speed correlation development. Experiments and simulation results were used for building up laminar flame speed correlation. Finally, experiments and simulations result also were used for validating the developed correlation.

5 Acknowledgments

The authors acknowledge the funding of TotalEnergies and ANRT under contract N°TOTAL U18-023 / CNRS-172041 / IFPEN 2018-0016.

6 Bibliography

[1] H. R. a. M. Roser, «Our world in data, Greenhouse gas emissions,» Global change data lab, [En ligne]. Available: https://ourworldindata.org/greenhouse-gas-emissions. [Accès le 27 05 2021].

[2] M. Ge, «World Greenhouse Gas Emissions: 2016,» World ressources institure, Washington DC, 2020.

[3] G. Kalghatgi, «Is it really the end of internal combustion engines and petroleum in transport?,» *Applied Energy,* vol. Volume 225, n° %1ISSN 0306-2619, pp. Pages 965-974, 2018.

[4] O. Colin, A. Pires da Cruz et S. Jay, «Detailed chemistry-based auto-ignition model including low temperature phenomena applied to 3-D engine calculations,» *Proceedings of the Combustion Institute,* vol. 30, n° %12, p. 2649–2656, 2005.

[5] S. Chevillard, O. Colin, J. Bohbot, M. Wang, E. Pomraning et P. K. Senecal, «Advanced Methodology to Investigate Knock for Downsized Gasoline Direct Injection Engine Using 3D RANS Simulations,» chez *SAE International400*, Warrendale, 2017.

[6] A. Comandini, N. Chaumeix, J. D. Maclean et G. Ciccarelli, «Combustion properties of n-heptane/hydrogen mixtures,,» *International Journal of Hydrogen Energy,* vol. 44 (3), pp. 2039-2052, 2019.

[7] R. Grosseuvres, A. Comandini, A. Bentaib et C. N., «Combustion properties of H2/N2/O2/steam mixtures,» *Proceedings of the Combustion Institute,* vol. 37 (2), pp. 1537-1546, 2019.

Correspondence to: outmane.mghanen@cnrs-orleans.fr

[8] D. Nativel, M. Pelucchi, A. Frassoldati, A. Comandini, A. C. N. C. E. Ranzi et T. Faravelli, «Laminar flame speeds of pentanol isomers: An experimental and modeling study,» *Combustion and Flame,* vol. 166, pp. 1-18, 2016.

[9] R. C. Eschenbach et J. T. Agnew, «Use of the constant-volume bomb technique for measuring burning velocity,» *Combustion and Flame,* vol. 2, n° %13, p. 273–285, 1958.

[10] P. D. Ronney et G. I. Sivashinsky, «A Theoretical Study of Propagation and Extinction of Nonsteady Spherical Flame Fronts,» *SIAM Journal on Applied Mathematics,* vol. 49, n° %14, p. 1029–1046, 1989.

[11] W. F., L. W., C. Z., J. Y. et L. C.K., «Uncertainty in stretch extrapolation of laminar flame speed from expanding spherical flames,» *Proceedings of the Combustion Institute,* vol. 35, n° %11, p. 663–670, 2015.

[12] W. C.K. et L. C.K., «On the determination of laminar flame speeds from stretched flames,» *Proceedings of the combustion institute,* vol. 20, n° %11, pp. 1941-1949, 1985.

[13] C. Zheng, «On the extraction of laminar flame speed and Markstein length from outwardly propagating spherical flames,» *Combustion and Flame,* vol. 158, n° %12, pp. 291-300, 2011.

[14] A. P. Kelley, J. K. Bechtold et C. K. Law, «Premixed flame propagation in a confining vessel with weak pressure rise,» *Journal of Fluid Mechanics,* vol. 691, pp. 26-51, 2012.

[15] A. Kelley et C. Law, «Nonlinear effects in the extraction of laminar flame speeds from expanding spherical flames,» *Combustion and Flame,* vol. 156, n° %19, pp. 1844-1851, 2009.

[16] J. Goulier, K. Bizon, N. Chaumeix, N. Meynet et G. Continillo, «Unsupervised analysis of experiments of laminar flame propagation in a spherical enclosure,» chez *AIP Conference Proceedings, 1790, ICCMSE 2016*, 2016.

[17] F. Wu, W. Liang, Z. Chen, Y. Ju et K. C., «Uncertainty in stretch extrapolation of laminar flame speed from expanding spherical flames,» *Proceedings of the Combustion Institute,* vol. 35, n° %11, pp. 663-670, 2015.

[18] H. Yu, W. Han, J. Santner, X. Gou, C. Sohn, Y. Ju et C. Z., «Radiation-induced uncertainty in laminar flame speed measured from propagating spherical flames,» *Combustion and Flame,* vol. 161, n° %111, pp. 2815-2824, 2014.

[19] P. Dagaut, A. Ristori, A. Frassoldati, T. Faravelli, G. Dayma et E. Ranzi, «Experimental and semi-detailed kinetic modeling study of decalin oxidation and pyrolysis over a wide range of conditions,» *Proceedings of the Combustion Institute,* vol. 34, n° %11, p. 289–296, 2013.

[20] R. Amirante, E. Distaso, P. Tamburrano et R. D. Reitz, «Laminar flame speed correlations for methane, ethane, propane and their mixtures, and natural gas and gasoline for spark-ignition engine simulations,» *International Journal of Engine Research,* vol. 18, n° %19, p. 951–970, 2016.

[21] Ö. L. Gülder, «Correlations of laminar combustion data for alternative SI engine fuels,» *SAE Technical Paper,* n°1841, 1984.

[22] F. H. V. Coppens, J. De Ruyck et A. A. Konnov, «The effects of composition on burning velocity and nitric oxide formation in laminar premixed flames of CH4+ H2+ O2+ N2,» *Combustion and Flame,* vol. 149, n° %14, pp. 409-417, 2007.

[23] S. Y. Liao, D. M. Jiang et Q. Cheng, «Determination of laminar burning velocities for natural gas,» *Fuel,* vol. 83, n° %19, p. 1247–1250, 2004.